JOURNAL OF SOLID STATE CHEMISTRY 95, 327–334 (1991)

Quarternary Oxide Phases $Ln_{4-x}A_{4+x}Co_{2+y}Al_{2-y}O_{15}$: The Structures of $Nd_{3.43}Ba_{4.42}Co_{2.23}Al_{1.77}O_{15}$ and $Y_2Sr_6Co_{2.08}Al_{1.92}O_{15}$

J. Y. LEE, J. S. SWINNEA, AND H. STEINFINK*

Center for Materials Science and Engineering and Department of Chemical Engineering, The University of Texas at Austin, Austin, Texas 78712

Received March 25, 1991

The crystal structure of two compounds having the generic formula $Ln_{4-x}A_{4+x}Co_{2+y}Al_{2-y}O_{15}$ has been determined. $Nd_{3.43}Ba_{4.42(1)}Co(Co_{1.23(6)}Al_{1.77})O_{15}$ (compound I), M_r = 1520.96, hexagonal, $P6_3mc$, a = 11.544(1) Å, c = 6.912(1) Å, V = 797.7(2) Å^3, Z = 2, D_x = 6.33 g cm^{-3}, Mo$K\alpha$ λ = 0.71069 Å, μ_l = 242.0 cm^{-1}; R = 0.045 for 758 reflections $>5\sigma(F)$. $Y_2Sr_6Co(Co_{1.08(6)}Al_{1.92})O_{15}$ (compound II), M_r = 1118.00, hexagonal, $P6_3mc$, a = 11.199(2) Å, c = 6.664(1) Å, V = 723.8(4) Å^3, Z = 2, D_x = 5.13 g cm^{-3}, MoK_α λ = 0.71069 Å, μ_l = 317.5 cm^{-1}; R = 0.076 for 373 reflections $>6\sigma(F)$. The structure consists of clusters formed by a Co–oxygen octahedron that shares three corners of a triangular face with three separate Co/Al–oxygen tetrahedra leading to a cluster formula $[Co^{VI}(Co/Al)_3^{IV}]O_{15}$. The tetrahedral interstice is randomly occupied by Co^{3+} and Al^{3+} ions. The octahedral interstice is occupied by Co whose valence is 2+ in compound I and 3+ in II. Two such clusters exist in the unit cell and they are joined by rare earth–alkaline earth cations in 6-fold (octahedral), 8-fold (bisdisphenoid), 10-fold (capped trigonal prism), and 12-fold (cubic close packed) coordination to the oxygen ions. The octahedral cation positions are randomly occupied by about equal amounts of Nd–Ba and Y–Sr, respectively. Phase I forms with Pr and Gd but not with La, Y, or Er, restricting its formation to lanthanide ionic radii between 1.14 and 1.06 Å.

Introduction

The discovery of compounds having superconducting transition temperatures in excess of 90 K has led to intensive research on the crystal chemistry of these phases. In particular the effect of isomorphous replacement of ions on the thermodynamic stability and physical properties has been studied in great detail. The phase $YSr_2Cu_3O_{7-\delta}$ cannot be prepared, but the substitution of Fe, Co, or Al, for Cu stabilizes this compound (*1*), although it is not a superconductor. These replacement reactions have occasionally produced new, unexpected phases such as $Sr_{5-x}Pb_{3+x}Cu_yO_{12-\delta}$ that formed while studying the substitution of Pb for Bi in $Bi_2(Sr_{1.5}Ca_{0.5})YCu_2O_8$ (*2*).

The superconducting and related phases are layer structures in which slabs of perovskite units are intercalated by blocks of fluorite, halite, Pb–Cu–Pb, and other moieties. Many can be considered derivatives of Ruddlesden–Popper phases, $Sr_{n+1}Ti_nO_{3n+1}$, where n is the number of perovskite layers separated by SrO halite-type layers (*3*). Numerous structures have been derived from the parent compounds with n = 1 to 3. Indeed, the p-type cuprate $La_{2-x}Sr_xCuO_4$ that

---

* To whom correspondence should be addressed.

0022-4596/91 $3.00

initiated the era of high-T_c superconductors, corresponds to the $n = 1$ phase in which the decreased valence of the dodecahedral ion is compensated by an increase in the valence of the octahedral ion. Recently a new phase, $Y_2SrFeCuO_{6.5}$, derived from the $n = 2$ parent has been synthesized by us (*4*). Relatively few compounds have been reported with structures based on the $n = 3$ motif, i.e., a layer of three octahedra formed by sharing of apical oxygen. We began a study of the hypothetical phase $(Ln_{4-x}Ba_x)(Cu_{3-y}Co_y)O_{10-\delta}$, Ln = Nd, but none of the numerous attempts produced such a compound. However, Weissenberg photographs of a small crystal selected from one of these reaction products was indexed on the basis of a hexagonal unit cell and appeared to be a new phase.

Superconducitivity has been observed in the compound $Pb_2Sr_2ACu_3O_8$ ($A = Ln$ or Ln + Sr or Ca) (*5*, *6*). We investigated the effect of transition metal substitution for Cu on the crystal structure and physical properties and attempted the synthesis of $Pb_2Sr_2Y Cu_2CoO_x$. The desired compound did not form. Single crystals were observed in some of the products and Weissenberg photographs of a small crystal showed it to be hexagonal. The cell parameters, space group, and relative intensities indicated that this compound was isostructural with the previously found unknown hexagonal phase in the Nd–Ba–Co–Cu system. We report here the crystal structure of this phase.

Experimental

A mixture of Nd_2O_3, $BaCO_3$, CuO, and Co_3O_4 to yield an oxide product of composition $Nd_2Ba_2Cu_2Co$, was placed in an alumina boat and heated at 1200°C for 12 hr. Subsequently the product was cooled at 1°/min to 900°C and then furnace cooled to room temperature. Black hexagonal rods were observed at the contact zone of the product with the alumina boat wall. Standardless EDX (energy dispersive X-ray spectroscopy) analysis showed the approximate composition of the crystals to be Nd : Ba : Co : Al = 2 : 2 : 1 : 1 and the absence of copper.

A mixture of PbO, $SrCO_3$, Y_2O_3, CuO, and Co_3O_4 to yield an oxide product of composition Pb_2Sr_2 YCu_2Co was placed into an alumina boat and heated at 1050°C for 6 hr. Controlled cooling at 3°/min followed the reaction. Black hexagonal rod-like crystals were observed on the surface of the reaction product which had melted and solidified against the wall of the boat. Standardless EDX analysis gave the approximate composition of the crystals as Y : Sr : Co : Al = 3 : 5 : 2 : 2; Pb and Cu were not present.

Single crystals of both phases were selected and oscillation, Weissenberg, and precession photographs showed both to be hexagonal with lattice parameters $a = 11.54$ Å, $c = 6.91$ Å for the Ba–Nd compound and $a = 11.2$ Å, $c = 6.66$ Å for the Y–Sr phase. Crystals of the Y–Sr phase were of poor quality and the crystal selected for data collection showed weak diffraction spots on Weissenberg photographs that were not from the main crystal. For both crystals the diffraction symmetry was $6/mmm$ and systematic absences occurred for $hh(\overline{2h})l$, $l = 2n + 1$, consistent with space groups $P6_3/mmc$, $P6_3mc$, and $P\overline{6}2c$.

In Table I are listed the conditions for the data collections and the results of the structure refinements. The lattice constants were obtained from a least-squares refinement of precisely determined 2θ values from 8 reflections in the range $26° < 2\theta < 29°$. For each reflection eight 2θ values were obtained from the permutation of ω, χ, ϕ, and 2θ. The intensity fluctuations of four standard reflections measured every 180 min were random and did not exceed 2.5%. Estimated standard deviations, $\sigma(F_0)$, were obtained from counting statistics. Absorption corrections were calculated with the pro-

TABLE I

SUMMARY OF DATA COLLECTION AND STRUCTURE REFINEMENT FOR $Nd_{3.43}Ba_{4.42(1)}Co_{2.23(6)}Al_{1.77}O_{15}$ (I) AND $Y_2Sr_6Co_{2.08(6)}Al_{1.92}O_{15}$ (II)

	I	II
Formula	$Nd_{3.43}Ba_{4.42(1)}Co_{2.23(6)}Al_{1.77}O_{15}$	$Y_2Sr_6Co_{2.08(6)}Al_{1.92}O_{15}$
Formula weight	1520.96	1118.00
Crystal system	Hexagonal	Hexagonal
a, Å	11.544(1)	11.199(2)
c, Å	6.912(1)	6.664(1)
V, Å^3	797.7(2)	723.8(4)
Space group	$P6_3mc$	$P6_3mc$
Z	2	2
D_x, g/cm^3	6.33	5.13
μ, cm^{-1}	242.0	317.5
λ, Å	0.71069	0.71069
$F(000)$	1313.1	1014.2
Dimensions, mm	0.16 × 0.018 × 0.018	0.20 × 0.068 × 0.054
Crystal faces	(00.1),(10.0),(01.0),(11.0)	(00.1),(10.0),(01.0),(11.0)
Diffractometer	Krisel Automated Picker	Krisel Automated Picker
Scan mode; speed deg min^{-1}	θ–2θ, variable for $\sigma(I)/I = .02$	ω, 3
scan width	$1 + 0.35 \tan\theta$	$1 + 0.35 \tan\theta$
Background		3 s at high and low ω
h, k, l range	0–14, 0–14, −9–9	−15–15, −15–15, 0–9
Maximum 2θ, deg	60	60
Measured reflections	1778	4413
Unique reflections	887	439
R_{int}	0.051	0.0507
Observed reflections	758 [$>5\sigma(F)$]	373 [$>6\sigma(F)$]
Absorption factor range	2.45–1.38	8.73–4.95
Number of variables	43	42
w^{-1}	$\sigma^2(F_o) + 0.0001F_o^2$	$\sigma^2(F_o) + 0.0001F_o^2$
S	1.56	2.08
Function minimized	$\Sigma w(F_o - F_c)^2$	$\Sigma w(F_o - F_c)^2$
R, wR	0.0445, 0.0411	0.0763, 0.0534
All data: R, wR	0.056, 0.046	0.100, 0.063
Max shift/esd	0.0000	0.0000
$\Delta\rho$, max. min eÅ^{-3}	5.2, −5.3	4.86, −8.7
Extinction parameter, g $F'_c = F_c[1 - (gF_c^2)(\sin\theta)^{-1}]$	$4.4(3) \times 10^{-7}$	$3.7(1) \times 10^{-7}$

gram ORABS (7); SHELX76 (8) was used for least-squares and electron density calculations. Atomic scattering factors, corrections for anomalous dispersion, and absorption cross sections were taken from the "International Tables for X-Ray Crystallography" (9). A semiempirical secondary extinction correction, g, was applied to calculated F with the expression $F'_c = F_c[1 - gF_c^2(\sin\theta)^{-1}]$.

The interpretation of results from direct methods and Patterson maps yielded the cation positions after the most probable space group was identified as $P6_3mc$. Fourier electron density and difference electron density maps revealed the oxygen atoms. Because the X-ray scattering factors of Nd, Ba, and Y, Sr are so similar it was not possible to assign these cation positions unequivocally. The variability of the cation–oxygen

TABLE II

POSITIONAL AND THERMAL DISPLACEMENT PARAMETERS $\times 10^4$, Å^2, FOR $Nd_{3.43}Ba_{4.42(1)}Co_{2.23(6)}Al_{1.77}O_{15}$ (I) AND $Y_2Sr_6Co_{2.08(6)}Al_{1.92}O_{15}$ (II)[a]

Atom	x	y	z	$U_{11} = U_{22}$	U_{33}	$U_{23} = -U_{13}$	U_{12}	U_{eq}
				I				
Nd	0.52331(6)	$\bar{x}$	0	83(4)	78(4)	−0(2)	53(4)	100(3)
Ba1	0.17219(7)	x	0.1744(3)	99(5)	137(6)	18(3)	35(6)	125(4)
Ba2	1/3	2/3	0.8691(4)	119(7)	79(12)	—	59(4)	133(6)
Ba3[b]	0	0	0.3569(6)	146(11)	312(23)	—	73(6)	228(10)
Co1	1/3	2/3	0.3245(10)	78(16)	89(27)	—	39(8)	99(13)
Co2/Al[c]	0.8227(2)	$\bar{x}$	0.1803(10)	83(17)	117(24)	−7(12)	31(19)	116(12)
O1	0.7579(9)	$2x$	−0.0014(36)	208(34)[d]				
O2	0.3964(11)	0.0696(12)	0.3115(17)	103(22)				
O3	0.9027(9)	$2x$	0.0833(24)	210(41)				
O4	0.5788(10)	$2x$	0.6718(34)	227(39)				
				II				
Y	0.5228(1)	$\bar{x}$	0	102(9)	115(14)	−12(7)	82(11)	124(8)
Sr1	0.1774(1)	x	0.1707(8)	115(11)	167(16)	37(8)	78(13)	141(8)
Sr2	1/3	2/3	0.8688(9)	137(16)	47(30)	—	69(8)	137(14)
Sr3	0	0	0.3382(10)	125(12)	46(29)	—	62(6)	120(12)
Co1	1/3	2/3	0.3210(17)	109(24)	253(56)	—	54(12)	181(24)
Co2/Al[e]	0.8258(3)	$\bar{x}$	0.1746(17)	129(26)	90(38)	13(18)	55(30)	139(22)
O1	0.7519(10)	$2x$	−0.0014(47)	177(46)				
O2	0.3918(18)	0.0646(18)	0.3064(31)	325(46)				
O3	0.9074(14)	$2x$	0.0754(47)	632(104)				
O4	0.5832(10)	$2x$	0.6682(46)	167(44)				

[a] The form of the anisotropic displacement parameters for the x-ray refinement is $\exp[-2\pi^2(U_{11}a^{*2}h^2 + \ldots 2U_{23}b^*c^*kl + \ldots)]$. U_{eq} is calculated from 1/3 of the trace of the diagonalized tensor.

[b] The site occupancy for Ba3 is 0.85(13). One half of the site is occupied by Ba(0.42), the other half by Nd(0.43).

[c] The site occupancy for Co_2 is 0.41(2) and Al is 0.59.

[d] The thermal displacement parameters for all oxygen atoms were obtained from isotropic refinements.

[e] The site occupancy for Co2 is 0.36(2) and Al is 0.64.

bond lengths and coordination polyhedra similarly presented obstacles to a definitive identification. A discussion of probable site occupancies is given in detail in the next section. The occupancies of the cations were permitted to vary during the refinement stages. The octahedral Co1 site converged to full occupancy, while the tetrahedral Co2 site converged to less than unity for phases I and II. Al was placed into that site so that the occupancy was $(Co2_{1-x}Al_x)$. The occupancies of Nd, Ba1, and Ba2 converged to unity but Ba3 contained an apparent vacancy. Similarly the occupancies of Y and the three crystallographically independent Sr converged to values that did not differ significantly from unity. The final positional parameters, thermal displacement parameters, and variable occupancy factors are listed in Table II. The refinement of the inverse structures (enantiomorphs) converged to somewhat higher R values and were rejected.

A Table of F_o, F_c and $\sigma(F_o)$ has been deposited.[1] Table III lists the X-ray powder diffraction pattern obtained with CuK_α and a diffractometer equipped with a diffracted beam monochromator from a product mix-

---

[1] See NAPS document No. 04895 for 5 pages of supplementary material. Order from ASIS/NAPS, Microfiche Publications, P.O. Box 3513, Grand Central Station, NY 10163. Remit in advance $4.00 for microfiche copy or for photocopy $7.75 up to 20 pages plus $.30 for each additional page. However, there is a billing and handling charge for this service of $15. Foreign orders add $4.50 for postage and handling, for the first 20 pages, and $1.00 for additional 10 pages of materials; $1.50 for postage of any microfiche orders.

TABLE III

Observed and Calculated *d* Spacings and Relative Intensities for the Powder X-ray Diffraction Pattern of $Nd_{3.6}Ba_{4.4}Co_{2.2}Al_{1.8}O_{15}$. The indexing is based on the hexagonal Cell a = 11.544(1) A, c = 6.912(1)A

h	*k*	*l*	*d* cal	*d* obs	*I* rel, cal	*I* rel, obs
0	2	0	5.000	4.994	8	5
0	2	1	4.051	4.046	18	16
1	2	1	3.316	3.314	27	25
0	1	2	3.266	3.260	7	7
0	3	1	3.002	3.009	10	11
1	1	2	2.965	2.960	28	25
2	2	0	2.887	2.889	100	100
0	2	2	2.843	2.838	53	50
1	3	1	2.574	2.574	3	3
1	2	2	2.550	2.549	11	12
0	3	2	2.399	2.398	30	30
0	4	1	2.350	2.353	15	17
2	3	0	2.293	2.298	2	2
0	1	3	2.245	2.241	8	7
2	2	2	2.215	2.216	1	3
2	3	1	2.177	2.180	8	8
1	3	2	2.163	2.162	2	4
0	2	3	2.092	2.091	4	3
1	4	1	2.080	2.080	7	6
0	4	2	2.025	2.026	20	19
1	2	3	1.967	1.980	2	2
0	5	1	1.921	1.924	10	12
2	3	2	1.911	1.913	3	3
0	3	3	1.895	1.894	2	3
1	4	2	1.845	1.846	18	18
2	4	1	1.823	1.825	5	5
1	5	0	1.796	1.796	2	2
1	3	3	1.772	1.771	3	3
1	5	1	1.738	1.741	1	3
0	5	2	1.731	1.733	5	6
0	1	4	1.703	1.711	1	2
0	4	3	1.694	1.694	2	2
3	3	2	1.681	1.683	5	5
0	6	0	1.666	1.669	12	12
2	4	2	1.658	1.660	10	12
2	3	3	1.625	1.626	10	10
3	4	1	1.599	1.602	7	7
2	5	1	1.560	1.563	7	7
0	3	4	1.534	1.534	6	5

Note. Additional lines above 60° 2θ.

ture to yield the composition $Nd_{3.6}Ba_{4.4}Co_{2.2}Al_{1.8}O_{15}$. The coordinates shown in Table II were used in the calculation.

Discussion

The X-ray scattering factors of Y, Sr, and Ba, Nd are so similar that only the Co/Al sites could be identified unequivocally. Even when the crystal structures were refined to acceptable *R* values, definitive atom designations of the four crystallographically independent Nd, Ba, and Y, Sr cation sites could not be made on the basis of bond lengths and oxygen coordination polyhedra. Probable compositions for the two crystals are based on several experimental results in addition to the crystallographic refinements. Systematic syntheses were carried out in which compositions were varied, and the reaction products were examined with powder X-ray diffraction procedures. The $Nd_{4-x}Ba_{4+x}Co_{2+y}Al_{2-y}O_{15}$ polycrystalline samples were synthesized from Nd_2O_3, $BaCO_3$, Al_2O_3, and Co_3O_4 over the composition range $-2 \leq x \leq 2$, $-1 \leq y \leq 1$. The samples were fired in air at 1200 to 1250°C for 48 hr with intermittent grinding. Within the limits of detectability of the X-ray powder diffraction technique single phase material formed for $0.4 \leq x \leq 1$ and $0.2 \leq y \leq 0.4$. When these values were exceeded, $BaAlO_{3-\delta}$ and $NdCoO_3$ were seen as additional phases. A similar procedure was used to study $Y_{4-x}Sr_{4+x}Co_{2+y}Al_{2-y}O_{15}$. Single phase material was observed when Co : Al was approximately 1 : 1, but the Y : Sr ratio had to be very close to 1 : 3. Even small deviations (±0.2) produced evidence of a second phase.

In compound I the sites labeled in Table II as Nd, Ba1, and Ba2 are essentially fully occupied by these ions. The Ba3 site is about 85% occupied on the basis of the least-squares refinement. Placing Nd into that site similarly yielded partial occupancy. The valence sum of 2.61 for this site indicates that Nd is also present. This crystallographic site, then, appears to contain about 15% vacancies and is shared equally between Ba and Nd. The results from the syntheses ex-

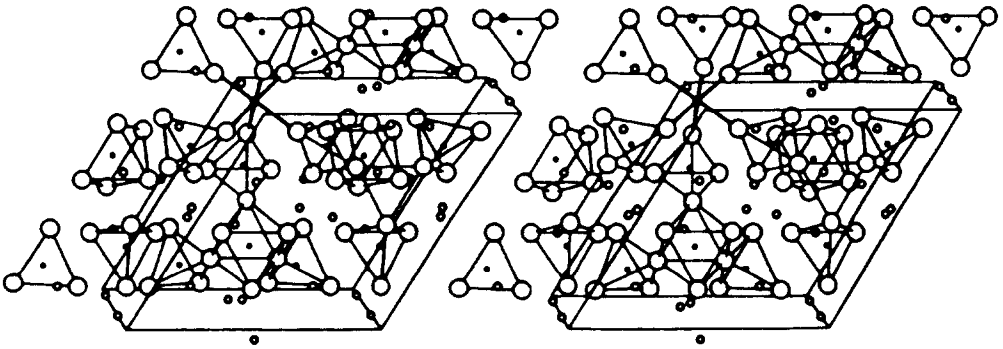

FIG. 1. Stereoscopic drawing (*11*) of the crystal structure of phase I. The octahedral environment of Ba3 is shown by bonds to six O3 ions that are part of six separate tetrahedra. The *a*-axis is horizontal and the *c*-axis points downward from the origin in the upper left corner. The line for the *c*-axis from 000 to 001 is omitted for the sake of clarity.

periments, bond lengths, and valence sum calculations (*10*) lead us to the conclusion that the composition of phase I is best represented by $Nd_{3.4}Ba_{4.4}\ \square_{0.2}Co_{2.23(6)}Al_{1.77}O_{15}$. The differences in calculated densities for small deviations from this formula are in the second decimal place and would not be detectable experimentally on the crystals that were available. In compound II the Y, Sr1, and Sr2 sites most likely are fully occupied by the respective ions, and the Sr3 site is shared by Sr and Y (valence bond sum 2.49). The best approximation to the composition of this crystal is $Y_2Sr_6Co_{2.08(6)}Al_{1.92}O_{15}$.

The sites labeled Nd and Y are in 8-fold coordination with oxygen ions at the vertices of a triangulated dodecahedron (bisdisphenoid), Fig. 2(a). Ba1 and Sr1 are in 10-fold coordination with the oxygen ions at the vertices of a slightly distorted trigonal prism whose rectangular faces and one triangular face are capped, Fig. 2(b). Ba2 and Sr2 are in 12-fold coordination with the oxygen ions forming a cubic close packed arrangement with the cation in the center of the plane of six oxygen ions, Fig. 2(c). Ba3 and Sr3 are in 6-fold coordination with oxygen ions at the vertices of an octahedron, Fig. 2(d). Figure 1 is a stereoscopic view of the structure, and one such Ba3 octahedron is shown. These sites contain a significant Nd, respectively Y, content.

In both phases, one Co ion is in an octahedral environment and a tetrahedral site is occupied by Co/Al. From valence bond calculations, Table IV, it can be seen that in compound I the octahedral Co is divalent while it is trivalent in phase II. Three oxygen ions O1 of the Co1 octahedron are shared with three separate Co2/Al tetrahedra to form a cluster, Fig. 1 and Fig. 2(e). These clusters are held together by the four crystallographically distinct heavy cations. Ba2 is above Co1 along the *c*-axis and the three unshared O4 ions at the corners of the triangular face of the octahedron constitute the A layer of the cubic close-packed arrangement. The three tetrahedra that share corners with the octahedron are arranged so that edges formed by two O2 from each tetrahedron form a hexagonal ring around Ba2, forming the B layer. The three O1 ions of the next Co1 octahedron (one *c*-axis dimension from the first Co1 octahedron) complete the C layer of the 12-fold coordination around Ba2.

Laterally the Co1–Co2/Al clusters are

linked by Ba3 in an octahedral interstice formed by six O3 from six separate tetrahedra. Ba1 and Nd fill 10-fold and 8-fold interstices, respectively, that exist between the octahedron–3 tetrahedra clusters that are formed by the c-glide operation in the unit cell.

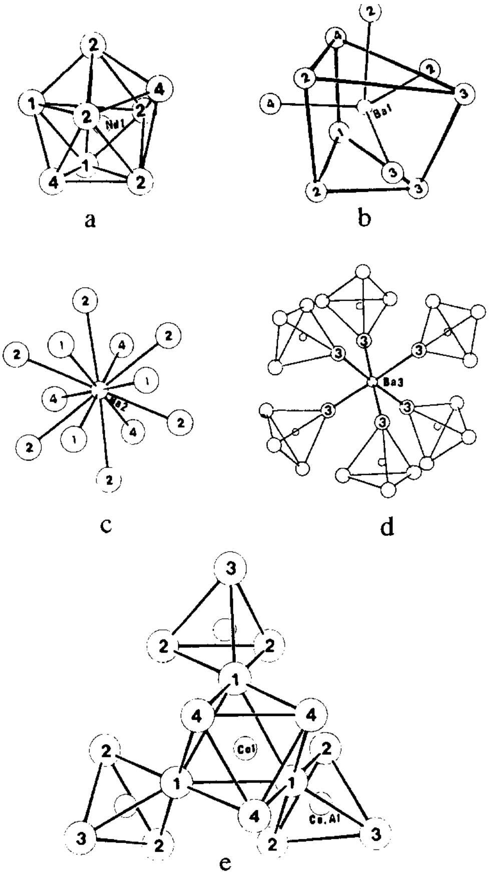

FIG. 2. Coordination polyhedra around cations in compounds I and II. (a) Nd, respectively Y, in 8-fold coordination formed by oxygen at corners of a bisdisphenoid. (b) Ba1, respectively Sr1, in 10-fold coordination; oxygen atoms at the corners of a trigonal prism, capping 3 quadrilateral and one triangular face. (c) Ba2, respectively Sr2, in 12-fold coordination; oxygen atoms in cubic close-packed array. (d) Ba3, respectively Sr3, in 6-fold coordination; 6 oxygen from 6 different tetrahedra are located at the corners of an octahedron. A Co1 octahedron sharing corners with 3 Co/Al tetrahedra to form the cluster Co $(Co/Al)_3$ O_{15}.

Phase I forms with Pr and Gd but not with La or Er, restricting its existence for lanthanide ionic radii between 1.14 and 1.06 Å. Phase II formed with Y and Sr; it did not form with Er. The Co2/Al–oxygen bond lengths are nearly the same in both phases but the Co1–oxygen bond lengths are longer in I than in II, reflecting the difference between the oxidation states of Co1 in the two phases. The oxygen framework is tightly packed. Five of the seven O1 near neighbor

TABLE IV

BOND LENGTHS (Å) WITH STANDARD DEVIATIONS IN PARENTHESES FOR COMPOSITIONS I AND II. THE NUMBERS IN BRACKETS ARE THE CALCULATED VALENCE SUMS

I		II	
Nd–2O1	2.513(13)	Y–2O1	2.430(13)
[2.88] 2O2	2.691(13)	[2.73] 2O2	2.584(30)
2O2	2.366(15)	2O2	2.298(32)
O4	2.526(21)	O4	2.502(26)
O4	2.363(20)	O4	2.342(23)
Ba1–O1	2.640(24)	Sr1–O1	2.580(28)
[1.94] 2O2	2.857(10)	[1.67] 2O2	2.724(22)
2O2	2.961(13)	2O2	2.861(32)
2O3	3.056(14)	2O3	3.048(19)
O3	3.198(18)	O3	3.159(31)
2O4	2.794(16)	2O4	2.622(12)
Ba2–3O1	3.144(23)	Sr2–3O1	2.970(28)
[1.86] 6O2	3.109(9)	[1.63] 6O2	3.073(19)
3O4	2.731(21)	3O4	2.570(5)
Ba3–3O3	2.713(18)	Sr3–3O3	2.509(31)
[2.61] 3O3	2.497(18)	[2.49] 3O3	2.393(31)
Co^{+2}1–3O4	2.048(20)	Co^{+3}1–3O4	1.913(24)
[1.92] 3O1	2.185(21)	[2.85] 3O1	2.034(25)
Co2/Al–O1	1.805(23)	Co2/Al–O1	1.852(26)
[2.77] 2O2	1.789(16)	[2.84] 2O2	1.764(33)
O3	1.734(19)	O3	1.715(31)
O1–2O1	3.160(31)	O1–2O1	2.864(34)
2O2	2.767(26)	2O2	2.719(38)
2O4	2.882(30)	O3	3.059(36)
O3	2.954(26)	2O2	3.295(35)
		2O4	2.743(35)
O2–O2	2.969(30)	O2–O2	2.941(66)
O3	2.960(19)	O3	2.923(43)
O2	3.195(29)	O2	3.147(51)
O4	3.087(21)	O4	3.044(36)
O4	2.942(28)	O4	2.888(37)
O4–2O4	3.040(35)	O4–2O4	2.804(38)

distances in I and seven of the nine near neighbor distances in II are essentially equal to the radius sum of the oxygen ionic radius. In I the large cations Nd and Ba in the interstices are a good fit with most ionic radius sums equal to or less than the cation–anion radii. However, this is not the case in II. Even though a contraction of the oxygen framework has occurred, the near neighbors around O1 increased to nine in II from seven in I; the interstices in which Sr1 and Sr2 are located provide a loose configuration and lead to some fairly long bond lengths. This is the reason for the apparent low valence bond sum for these ions. It also explains the dependence of phase I formation on the lanthanide ionic radius.

The idealized stoichiometries for I and II are, respectively, $(Nd_4Ba_4)Co(CoAl_2)O_{15}$ and $(Y_2Sr_6)Co(CoAl_2)O_{15}$, with Co^{2+} in the octahedral site in I and Co^{3+} in II. Charge balance is achieved by small variations in the lanthanide : alkaline earth ratio and probably also by vacancies.

Acknowledgment

This research was supported by the R. A. Welch Foundation, Houston, Texas.

References

1. S. A. Sunshine, L. F. Schneemeyer, T. Siegrist, D. C. Douglass, J. V. Waszczak, R. J. Cava, E. M. Gyorgy, and D. W. Murphy, *Chem. Mater.* **1,** 331 (1989).
2. J. S. Kim, X. X. Tang, A. Manthiram, J. S. Swinnea, and H. Steinfink, *J. Solid State Chem.* **85,** 44 (1990).
3. S. N. Ruddlesden and P. Popper, *Acta Crystallogr.* **11,** 54 (1958).
4. J. S. Kim, J. Y. Lee, J. S. Swinnea, H. Steinfink, W. M. Reiff, P. Lightfoot, S. Pei, and J. D. Jorgensen, *J. Solid State Chem.* **90,** 331 (1991).
5. M. A. Subramanian, J. Gopalakrishnan, C. C. Torardi, P. L. Gai, E. D. Boyes, T. R. Askew, R. B. Flippen, W. E. Farneth, and A. W. Sleight, *Physica C.* **157,** 124 (1989).
6. R. J. Cava, B. Batlogg, J. J. Krajewski, L. W. Rupp, L. F. Schneemeyer, T. Siegrist, R. B. van Dover, P. Marsh, W. F. Peck, Jr., P. K. Gallagher, S. H. Glarum, J. H. Marshall, R. C. Farrow, J. V. Waszczak, R. Hull, and P. Trevor, *Nature (London)* **336,** 211 (1988).
7. D. J. Wehe, W. R. Busing, and H. A. Levy, "Program ORABS, ORNL, TM 229," Oak Ridge, TN (1962).
8. S. M. Sheldrick, "SHELX 76, Program for Crystal Structure Determination," University of Cambridge, England (1976).
9. "International Tables for X-Ray Crystallography," Vol. IV, Kynoch Press, Birmingham (1974). (Present distributor Kluwer Academic Publishers, Dordrecht).
10. I. D. Brown and D. Altermatt, *Acta Crystallogr., Sect. B* **41,** 244 (1985).
11. C. K. Johnson, "ORTEP, Report ORNL-5138," Oak Ridge, TN (1976).